PROCEEDINGS, Thirty-Second Workshop on Geothermal Reservoir Engineering
Stanford University, Stanford, California, January 22-24, 2007
SGP-TR-183

WATER INJECTION AS A MEANS FOR REDUCING NON-CONDENSIBLE AND CORROSIVE GASES IN STEAM PRODUCED FROM VAPOR-DOMINATED RESERVOIRS

Karsten Pruess, Nicolas Spycher and Timothy J. Kneafsey

Earth Sciences Division, Lawrence Berkeley National Laboratory
Berkeley, CA 94720
e-mail: K_Pruess@lbl.gov

ABSTRACT

Large-scale water injection at The Geysers, California, has generated substantial benefits in terms of sustaining reservoir pressures and production rates, as well as improving steam composition by reducing the content of non-condensible gases (NCGs). Two effects have been recognized and discussed in the literature as contributing to improved steam composition, (1) boiling of injectate provides a source of "clean" steam to production wells, and (2) pressurization effects induced by boiling of injected water reduce upflow of native steam with large NCG concentrations from depth. In this paper we focus on a possible additional effect that could reduce NCGs in produced steam by dissolution in a condensed aqueous phase.

Boiling of injectate causes pressurization effects that will fairly rapidly migrate outward, away from the injection point. Pressure increases will cause an increase in the saturation of condensed phase due to vapor adsorption on mineral surfaces, and capillary condensation in small pores. NCGs will dissolve in the additional condensed phase which, depending upon their solubility, may reduce NCG concentrations in residual steam.

We have analyzed the partitioning of HCl between vapor and aqueous phases, and have performed numerical simulations of injection into superheated vapor zones. Our simulations provide evidence that dissolution in the condensed phase can indeed reduce NCG concentrations in produced steam.

INTRODUCTION

Vapor-dominated geothermal reservoirs such as The Geysers, California, are by their very nature water-short systems. Connate waters provide an inventory of heat transmission fluid that is insufficient for extracting more than a fraction of stored heat. Large-scale production at The Geysers with inadequate fluid replacement by injection led to strong declines in reservoir pressures and well flow rates during the 1980s and early 1990s (Sanyal et al., 2000). The installed electric generating capacity peaked around 1990 at about 2,000 MW and subsequently declined. A systematic program of increasing injection has been implemented, that uses condensate from the cooling towers, local creek water, and recycled waste water from neighboring communities that is sent by pipeline to The Geysers. The SEGEP pipeline from Lake and Sonoma counties is capable of delivering up to 36,000 metric tons of water per day (Smith et al., 2000). The Santa Rosa Geysers Recharge Project (SRGRP) provides as much as 42,000 metric tons of tertiary-treated municipal wastewater via a 65-km pipeline from Santa Rosa (Stark et al., 2005). Injection has been shown to provide pressure support to the reservoir, and has provided additional benefits by reducing the concentration of non-condensible gases (NCGs). In addition to reducing corrosion problems in wellbores and surface lines, lowering of NCG concentrations has provided substantial improvements in energy conversion efficiency (Stark and Koenig, 2001).

Reductions in NCG concentrations have been attributed to two effects, (1) boiling of injectate provides a source of "clean" steam to production wells, and (2) pressurization from boiling of injected water reduces upflow of native steam with large NCG concentrations from depth. This paper focusses on a possible third effect, namely, in situ removal of highly water-soluble NCGs, such as HCl, by dissolution in a condensed aqueous phase.

THEORETICAL CONSIDERATIONS

Truesdell and coworkers noted that "large-scale reinjection, generating or replenishing liquid saturation … could theoretically scrub HCl before it enters the wellbore" (Haizlip and Truesdell, 1989), and pointed out that HCl will be scrubbed from HCl-bearing steam if it "encounters liquid with higher pH,

lower temperature, or lower salinity" (Truesdell et al., 1989). These observations lead to the suggestion that HCl and other NCGs in Geysers steam may be removed *in situ* by means of appropriately placed water injection. However, although conceptually simple, a "literal" implementation of this idea seems unworkable, because in practice it would not be possible to control where the injected liquid goes, so that the idea of placing water in the path of steam flowing to the production wells seems unrealistic. However, it may be possible to achieve removal of NCGs *in situ* even if no specific control can be exerted on the migration of injected water. Injected water will be heated by contact with the reservoir rocks and will partially vaporize when its temperature reaches the saturation temperature at prevailing reservoir pressures. The vaporization will cause volume expansion and pressurization that will propagate fairly rapidly outward, away from the injection plume. Liquid saturations will then increase throughout the volume in which steam pressures rise, by a combination of vapor adsorption on mineral surfaces and condensation effects in small capillaries (Pruess and O'Sullivan, 1992). This well-known phenomenon is quantitatively described by Kelvin's equation, which expresses vapor pressure as a function of temperature and liquid saturation,

$$P_{vap}\left(T,S_{liq}\right) = f_{VPL}\left(T,S_{liq}\right)\cdot P_{sat}\left(T\right) \qquad (1)$$

Here

$$f_{VPL} = \exp\left[\frac{M_w\, P_{suc}\left(S_{liq}\right)}{\rho_{liq}\, R\left(T+273.15\right)}\right] \qquad (2)$$

is the vapor pressure lowering (VPL) factor. P_{sat} is the saturated vapor pressure of bulk aqueous phase, the "suction pressure" $P_{suc} < 0$ is the difference between aqueous and gas phase pressures, ρ_{liq} is liquid density, M_w is the molecular weight of water, R is the universal gas constant, and T is temperature in ^{o}C. "Suction pressure" P_{suc} is a phenomenological concept that includes conventional capillary pressures, as well as pressures generated by adsorption of liquid water on hydrophilic mineral surfaces. When the ratio P_{vap}/P_{sat} increases due to pressurization from injection-derived steam (IDS), we have f_{VPL} ==> 1 from Eq. (1), and P_{suc} ==> 0 from Eq. (2), to which corresponds an increasing amount of condensed phase. The additional condensed (liquid) phase formed can dissolve NCGs. Under certain conditions (see below) the partitioning of NCGs between gas and liquid phases may be described by Henry's law.

$$P_{NCG} = K_H \cdot x_{NCG} \qquad (3)$$

Here, P_{NCG} is the partial pressure of the NCG, K_H is Henry's coefficient (same units as P_{NCG}), and x_{NCG} is the mole fraction of NCG dissolved in the liquid phase. Henry's coefficient describes partitioning of a volatile and water-soluble compound between two phases and can be regarded as an inverse solubility. It is a function of temperature and also depends on the composition and state of tension (suction pressure) of the condensed aqueous phase. Typical values of Henry's coefficient for pure water (no salinity) are of order 10^{10} Pa for a sparingly soluble gas such as nitrogen, $5x10^{8}$ Pa for CO_2, and 10^{5} Pa or less for highly soluble gases.

The propagation of vapor pressure increases outward from the injection plume is described by a parabolic (diffusive) equation, suggesting that it may be possible to increase condensed phase saturations broadly, throughout a large region. Such condensed phase may be effective in dissolving highly soluble corrosive gases such as HCl. To achieve this effect it will not be necessary to place the actual injection water into the pathway of the steam towards the production wells. Once the HCl is dissolved, additional beneficial effects may be derived from chemical interactions with rock minerals that would buffer the acidity.

GAS SOLUBILITY

Previous studies on solubility of HCl at conditions of interest for vapor-dominated reservoirs were made by Truesdell et al. (1989), extrapolating experimental data obtained for temperatures T ≤ 110 ˚C. Here we derive HCl solubilities at higher temperatures using standard chemical equilibrium concepts and more recent thermodynamic data as incorporated into the program SUPCRT92 (Johnson et al., 1992).

For non-reactive and sparingly soluble gases, partitioning between gas and liquid phases can be described by Henry's law (Eq. 3). The basic chemical equilibrium for HCl partitioning between aqueous and gas phases is written as

$$HCl_{(g)} \Leftrightarrow HCl_{(aq)} \qquad (4)$$

with the equilibrium (solubility) constant

$$K = a_{HCl(aq)}/F_{HCl(g)} \qquad (5)$$

Here, $a_{HCl(aq)} = \gamma_{HCl(aq)} m_{HCl(aq)}$ is the activity (effective concentration), expressed in terms of the activity coefficient γ and the molality m. $F_{HCl(g)} = \Phi_{HCl(g)} P_{HCl(g)}$ is the fugacity (effective pressure), with Φ the fugacity coefficient, and P the partial pressure.

Assuming pure water and ideal behavior in the gas phase, we have $\gamma \approx 1$, $\Phi \approx 1$, so that

$$K \approx m_{HCl(aq)}/P_{HCl(g)} \quad (6)$$

Eq. (6) has the form of Henry's law, with solubility K being an inverse Henry's coefficient. Aqueous HCl may dissociate according to

$$HCl_{(aq)} \Leftrightarrow H^+ + Cl^- \quad (7)$$

with a dissociation equilibrium constant of

$$K_1 \approx m_{H+}m_{Cl-}/m_{HCl(aq)} \quad (8)$$

where we again assumed activity coefficients equal to 1, so that molalities may be used instead of activities. Equilibrium constants for Eqs. (6, 8) for a range of (T, P)-conditions are given in Table 1, as obtained from SUPCRT92 (Johnson et al., 1992).

Table 1. Equilibrium constants for reactions Eq. (4, 7) from SUPCRT92 (Johnson et al., 1992).

T (^{o}C)	P (bar)	log(K)	log(K_1)
0.01	1.013	6.958	0.513
25	1.013	5.596	0.71
60	1.013	4.083	0.802
100	1.013	2.754	0.748
150	4.757	1.513	0.518
200	15.537	0.605	0.142
250	39.736	-0.044	-0.39
300	85.838	-0.45	-1.169

To proceed further we assume that pH will be constrained by interactions between the fluids and assemblages of reactive minerals. For example, Haizlip and Truesdell (1988) suggested that pH of aqueous phase at The Geysers may be buffered at near-neutral values by reactions between feldspars and micas. Substituting $m_{H+} = 10^{-pH}$, Eq. (8) gives

$$m_{Cl-} = K_1 m_{HCl(aq)} 10^{pH} \quad (9)$$

so that total aqueous HCl concentration becomes $m_{HCl(aq,tot)} = m_{HCl(aq)}\left(1 + K_1 10^{pH}\right)$ and, substituting into Eq. (6),

$$P_{HCl(g)} = \frac{1}{K\left(1 + K_1 10^{pH}\right)} m_{HCl(aq,tot)} \quad (10)$$

Substituting $m_{HCl(aq,tot)} = 55.5 x_{HCl}/(1 - x_{HCl})$, with x_{HCl} the total mole fraction of (associated and dissociated) HCl, Eq. (10) has for $x_{HCl} << 1$ the form of Henry's law Eq. (3), with Henry's coefficient given by

$$K_H = \frac{55.5}{K\left(1 + K_1 10^{pH}\right)} \quad (11)$$

Thus, under conditions where pH is strictly constrained by mineral reactions, Henry's law is applicable to HCl dissolution.

Relationships between $P_{HCl(g)}$ and aqueous HCl concentration, expressed as mole fraction x_{HCl}, are plotted in Fig. 1. For comparison Fig. 1 also includes P_{HCl} for a hypothetical Henry's coefficient of K_H = 1 bar, corresponding to a pH = 2.17 according to Eq. (11). HCl solubilities increase strongly (K_H decreases) with decreasing temperature and increasing pH (Figs. 2, 3).

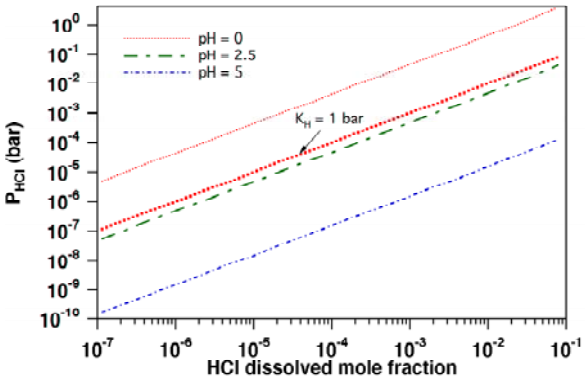

Figure 1. HCl partial pressures at 250 ^{o}C for different pH. The line labeled K_H = 1 bar refers to a (hypothetical) Henry's coefficient of 1 bar.

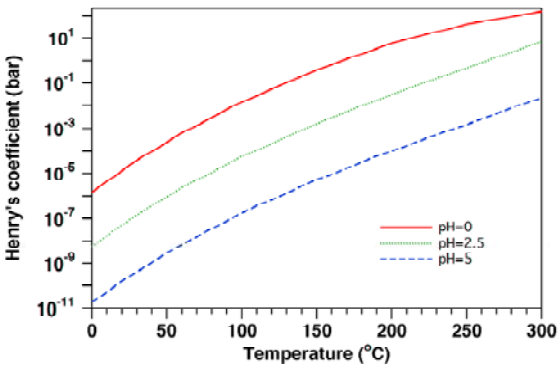

Figure 2. Henry's coefficient for HCl dissolution in pure water under pH-constrained conditions as function of temperature.

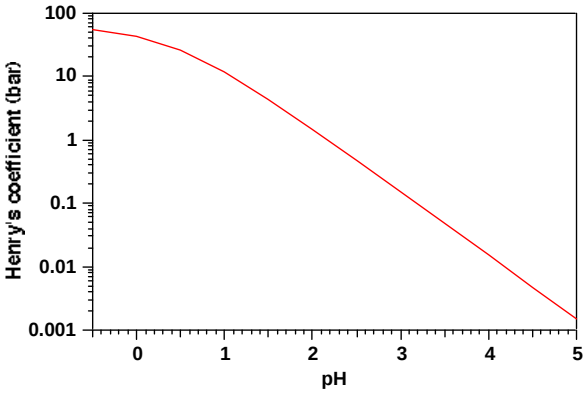

Figure 3. Henry's coefficient for HCl dissolution in pure water under pH-constrained conditions at T = 250 °C.

The derivations given above assumed that pH was constrained by mineral buffers, and were made for a "bulk" (free) aqueous phase. HCl solubility may be different when pH is not constrained by rock-fluid interactions, and when the solvent is not a free aqueous phase, but is a condensed phase that is held under tension in porous media, comprising vapor adsorbed on mineral surfaces as well as water condensed in small capillaries (Lassin et al., 2005). We are currently assembling a laboratory experimental facility to study condensation and dissolution phenomena at pressures below saturated vapor pressure, in order to determine the partitioning of HCl between vapor and a condensed phase held under tension.

SIMULATION STUDIES

Problem Setup

Numerical simulations of water injection and steam production were performed using an idealized five-spot well configuration as shown in Figure 4. The same setup had been employed in previous studies of reservoir processes at The Geysers, and similar reservoir parameters were used here as in earlier studies (Pruess, 2002). A five-spot configuration is commonly used for studies of geothermal production and injection (Sanyal and Butler, 2005), even though in reality injection and production wells will rarely if ever be arranged in such a regular pattern. The geometric idealization of the five-spot configuration has a high degree of symmetry, allowing to focus on a reservoir subdomain of limited spatial extent, so that reasonable spatial resolution can be achieved without requiring an inordinately large numbers of grid blocks. Because of symmetry, only 1/8 of the basic five-spot pattern needs to be modeled, and a 5-point parallel grid (Pruess, 1991) of 196 square blocks with 10.88 m length was used to represent one

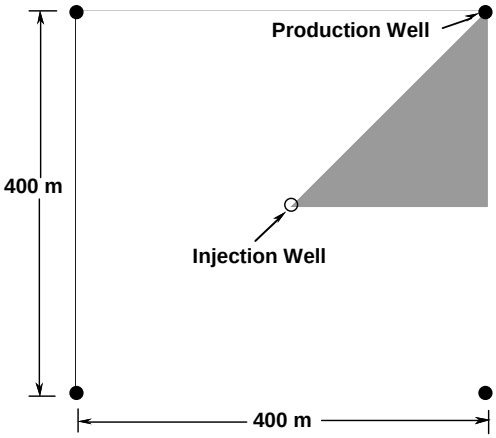

Figure 4. Schematic of five-spot production-injection system, with shading showing a 1/8 symmetry element.

layer of this 1/8 symmetry element. Reservoir thickness was 500 m, which for our 3-D simulations was divided into five layers of 100 m thickness each, for a total of 5x196 = 980 grid blocks. The simulations presented here used a single porous medium description for the reservoir; studies for a fractured reservoir description using the method of "multiple interacting continua" (MINC; Pruess and Narasimhan, 1985) were also made (Pruess, 2006).

Table 2 lists reference parameters used for the model; constant conditions of (T, P) = (250 ˚C, 30 bar) are employed at the lower boundary to represent a depleted reservoir zone that is fed by steam rising from depth. Production is specified by maintaining constant pressure conditions in the production grid blocks (top three layers). For the 10.88 m grid spacing used here this corresponds to an effective wellbore radius of 6.14 m, or a skin factor of - 4.1 for an 8'' well (r_w = 4'' = 10.16 cm), a value that is not unreasonable for wells at The Geysers. Flowing bottomhole pressure is specified as 8 bar opposite the top layer of the model. Initial conditions for this case were prepared by running the system to steady state, resulting in a production rate of 6.56 kg/s (full well basis) and conditions of (T, P) ≈ (225 ˚C, 15 bar) in the top layer, with a liquid saturation of $S_l \approx 4$ %. Injection is then made at a rate of 40 kg/s (full well basis). The possibility that liquid water may be trapped in the tight matrix rock is accounted for by specifying a large irreducible water saturation of 80 %. Some variations of the reference parameters were explored, as was behavior of non-condensible gases with a range of solubilities in the aqueous phase (see "Results" section, below). All simulations reported here were made with our general-purpose reservoir simulator TOUGH2 and the EOS4 fluid property module for water-NCG mixtures including VPL

Table 2. Specifications of five-spot single-porosity reservoir problem

Reservoir properties	
Horizontal permeability	43.2×10^{-15} m^2
Porosity	4 %
Thickness	500 m
Vertical permeability	43.2×10^{-15} m^2 (top 300 m) 10×10^{-15} m^2 (bottom 200 m)
Relative permeability liquid: van Genuchten (1980); parameters gas: Corey (1954); parameter	 $\lambda = 0.4438$; $S_{lr} = 0.80$ $S_{gr} = 0.05$
Capillary pressure van Genuchten (1980); parameters	 $\lambda = 0.4438$; $S_{lr} = 0$; $P_0 = 17.27 \times 10^5$ Pa
Pattern area	160,000 m^2 (= 39.5 acres)
Well spacing (distance from injector to producer)	282.8 m (928.0 ft)
Initial production rate (full well basis)	10.45 kg/s
Injection[#] rate (full well basis)[&] enthalpy	40 kg/s 100 kJ/kg
Initial conditions	steady state (see text)

[#] injection well is assumed open in the top layer only.

[&] "full well basis" means rate for the entire well, which is 8 times the value used in the 1/8 symmetry domain considered in our model.

effects (Pruess et al., 1999; Pruess, 2004). Special enhancements were implemented to allow modeling of NCGs with different molecular weight and aqueous solubility.

Results

As the injected water migrates outward, away from the injection point, it is being heated and partially vaporized by contact with the reservoir rocks. Fig. 5 shows the complex non-monotonic behavior of fluid pressures resulting from injection. Along a line from the injection to the production point (going from right to left in Fig. 5), there initially is a strong pressure decline. Then a local minimum is reached, followed by pressure increase and a local maximum, and subsequently there is a gradual decline towards the production well. Over time this pattern persists and moves away from the injector.

The pressure behavior arises from an interplay of single-phase liquid flow near the injection well with two-phase steam-water flow under non-isothermal conditions at larger distance. In the region with steep pressure gradients around the injector we have single-phase liquid. Pressure gradients increase in this region over time, due to strong increases in water viscosity as temperatures decline from continued injection. The local minimum in pressure occurs at the outer boundary of the single-phase liquid region (compare water saturations in Fig. 6). At larger

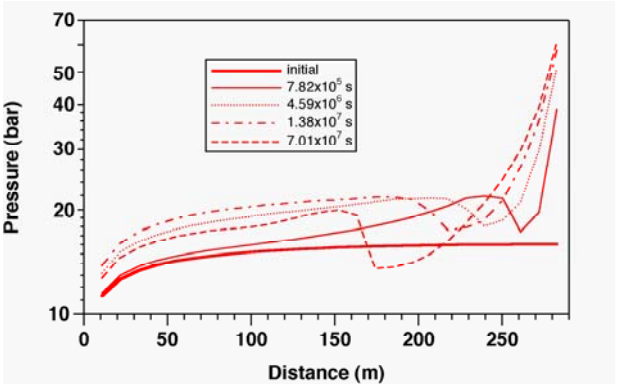

Figure 5. Pressure profiles at different times in the top reservoir layer along a line extending from the injection well (at 282.8 m) to the production well (at 0 m).

distance from the injector two-phase water-steam conditions are present. The inner portion of the two-phase zone is cooled by injected water. The cooling is most pronounced closest to the injection plume, and becomes weaker at increasing distance from the injection well.

Water saturations generally decrease with increasing distance from the injection point (Fig. 6). At larger distance from the injection point, associated vapor pressure lowering effects (declining f_{VPL} coefficient in Eq. 2 as water saturation decreases) become

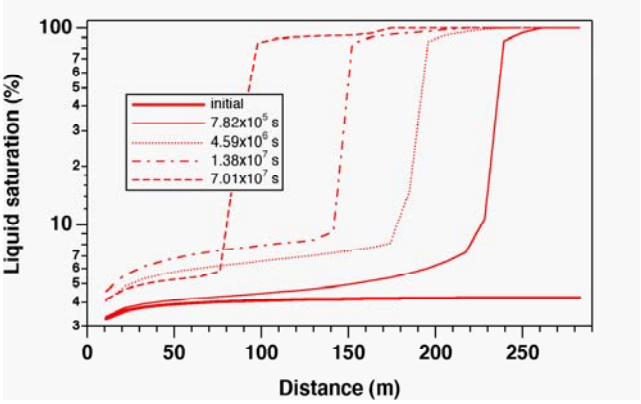

Figure 6. Liquid saturation profiles at different times in the top reservoir layer along a line extending from the injection well (at 282.8 m) to the production well (at 0 m).

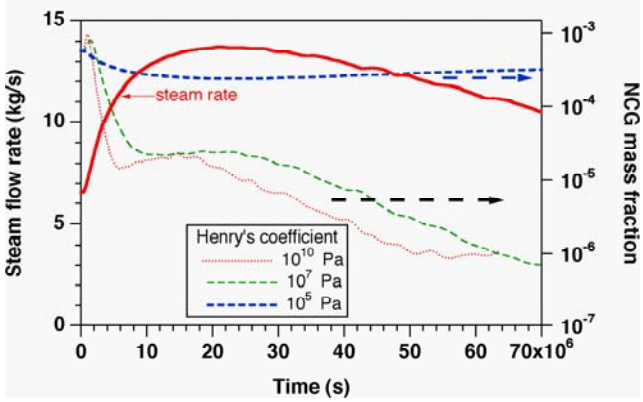

Figure 7. Steam production rate (full-well basis) and NCG mass fractions in produced steam for NCGs with different solubilities.

stronger than increases in saturated vapor pressure due to increasing temperatures, giving rise to a local maximum in vapor pressure. Beyond the local pressure maximum there is a monotonic pressure gradient towards the production well. In the region between the local maximum and local minimum in pressure, steam flows towards rather than away from the injection point. Liquid phase pressures decline monotonically away from the injection point, due to capillary pressure gradients that are stronger than the increases in steam pressure. Thus, liquid water flows away from the injection point everywhere. In the inner (near-injector) portion of the two-phase zone, we have a steam-water counterflow, with water flowing away from and steam flowing towards the injection point. The steam flowing towards the liquid portion of the injection plume condenses there, depositing its latent heat of vaporization and heating injected water.

The steam production rate shows a non-monotonic behavior, more than doubling over the first 20×10^6 s (0.63 yr), and then slowly declining (Fig. 7). The increase is due to boiling of injectate, while the subsequent decline is due to a slow decrease in temperature over the surface of the expanding injection plume and associated pressure decrease. Fig. 7 also shows NCG mass fractions in produced steam, for three different values of NCG solubility (Henry's coefficient). For modeling NCG behavior, the initial (pre-injection) steady state was prepared by specifying a small, constant NCG partial pressure at the bottom boundary, typically in the range of 10 – 1000 Pa. Steam flow rates are not affected by the presence of such small concentrations of NCG. For the lower-solubility gases ($K_H = 10^{10}$ and 10^7 Pa), injection gives rise to a brief small increase in NCG concentration, followed by a steep decline. For a high-solubility NCG ($K_H = 10^5$, corresponding to HCl solubility at pH = 2.17; cf. Fig. 3) the decline is monotonic but weaker, and long-term NCG concentrations remain much higher. These outcomes can be readily understood as follows. For NCGs with low aqueous solubility, the partial steam condensation induced by injection-derived pressurization (Fig. 5) will leave the residual steam enriched in NCGs and will increase NCG concentrations in produced steam. Such increase is temporary, however, because over time an increasing fraction of produced steam is derived from vaporization of injected water, which is low in NCGs. For NCGs with large solubility, pressurization-induced condensation will cause substantial dissolution of NCGs, and will reduce NCG concentrations in residual steam. Long-term NCG concentrations in produced steam remain higher for more soluble NCGs, however, because there is a larger inventory dissolved in the condensed phase that continues to supply NCGs to the steam through slow evaporation.

CONCLUDING REMARKS

Water injection reduces NCG concentrations in steam due to three different mechanisms, (1) providing a source of "clean" steam low in NCGs, (2) reducing upflow of native steam with larger NCG concentrations, and (3) generating additional condensed phase that provides for *in situ* scrubbing of water-soluble NCGs. The latter mechanism has not been studied much and is the main focus of this paper.

We have presented a theoretical framework and numerical simulation capabilities for analyzing reservoir pressurization from injection-derived steam (IDS) and associated vapor adsorption and capillary condensation effects. HCl dissolution into condensed

phase was discussed in terms of thermodynamic equilibrium concepts, and assuming pH to be constrained by mineral buffers.

Preliminary 3-D numerical simulations have demonstrated significant vapor pressure increases from injection, condensation effects arising from the pressurization, and NCG dissolution effects in the condensed phase. More specifically, it was shown that injection-induced condensation effects will increase concentrations of NCGs with low solubility in residual steam, while decreasing concentrations of highly soluble NCGs. Long-term steam composition effects are complicated by the fact that condensed aqueous phase can be both a sink for and a source of NCGs: more soluble NCGs are scrubbed from steam more effectively, but also have a larger dissolved inventory. These effects form possible building blocks for achieving *in situ* abatement of NCGs, which is the central objective of the present project. Future studies will investigate possibilities and limitations for using targeted water injection to control NCGs, and to aid in design and interpretation of laboratory experiments that are currently being assembled.

ACKNOWLEDGEMENT

Thanks are due to Mack Kennedy for a review of the manuscript. This work was supported by a PIER grant from the California Energy Commission (CEC) and by the Assistant Secretary for Energy Efficiency and Renewable Energy, Office of Geothermal Technologies, of the U.S. Department of Energy under Contract No. DE-AC02-05CH11231.

REFERENCES

Corey, A.T. The Interrelation Between Gas and Oil Relative Permeabilities, *Producers Monthly*, pp. 38 - 41, November 1954.

Haizlip, J.R. and A.H. Truesdell. Hydrogen Chloride in Superheated Steam and Chloride in Deep Brine at The Geysers Geothermal Field, California, in: *Proceedings, Thirteenth Workshop on Geothermal Reservoir Engineering*, report SGP-TR-113, pp. 93–99, 1988.

Haizlip, J.R. and A.H. Truesdell. The Correlation of Noncondensible Gas and Chloride in Steam at The Geysers, *Trans., Geoth. Resour. Counc.*, Vol. 13, pp. 455–460, 1989.

Johnson, J.W., E.H. Oelkers and H.C. Helgeson. SUPCRT92: A Software Package for Calculating the Standard Molal Thermodynamic Properties of Minerals, Gases, Aqueous Species, and Reactions from 1 to 5000 bars and 0 to 1000 degrees C: *Computers and Geosciences*, v. 18, p. 899–948, 1992.

Lassin, A., M. Azaroual and L. Mercury. Geochemistry of Unsaturated Soil Systems: Aqueous Speciation and Solubility of Minerals and Gases in Capillary Solutions, *Geochim. Cosmochim Acta*, Vol 69, No. 22, pp. 5187–5201, 2005.

Pruess, K. Grid Orientation and Capillary Pressure Effects in the Simulation of Water Injection into Depleted Vapor Zones, *Geothermics*, Vol. 20, No. 5/6, pp. 257 - 277, 1991.

Pruess, K. Numerical Simulation of Multiphase Tracer Transport in Fractured Geothermal Reservoirs, *Geothermics*, Vol. 31, pp. 475 - 499, 2002.

Pruess, K. The TOUGH Codes—A Family of Simulation Tools for Multiphase Flow and Transport Processes in Permeable Media, *Vadose Zone J.*, Vol. 3, pp. 738 - 746, 2004.

Pruess, K. Numerical Modeling of Water Injection into Vapor-Dominated Geothermal Reservoirs, Lawrence Berkeley National Laboratory, report LBNL-61917, August 2006.

Pruess, K. and T.N. Narasimhan. A Practical Method for Modeling Fluid and Heat Flow in Fractured Porous Media, *Soc. Pet. Eng. J.*, 25 (1), 14-26, February 1985.

Pruess, K. and M. O'Sullivan. Effects of Capillarity and Vapor Adsorption in the Depletion of Vapor-Dominated Geothermal Reservoirs, presented at Seventeenth Workshop on Geothermal Reservoir Engineering, Stanford University, Stanford, CA, January 1992.

Pruess, K., C. Oldenburg and G. Moridis. TOUGH2 User's Guide, Version 2.0, Lawrence Berkeley National Laboratory Report LBNL-43134, Berkeley, CA, November 1999.

Sanyal, S.K., S.J. Butler, P.J. Brown, K. Goyal, and T. Box. An Investigation of Productivity and Pressure Decline Trends in Geothermal Steam Reservoirs, *Proceedings, World Geothermal Congress 2000*, pp. 873 - 877, International Geothermal Association, May-June 2000.

Sanyal, S.K. and S.J. Butler. An Analysis of Power Generation Prospects from Enhanced Geothermal Systems, *Proceedings, Paper 1632.pdf*, World Geothermal Congress 2005, Antalya, Turkey, 24-29 April 2005.

Smith, B., J. Beall and M. Stark. Induced Seismicity in the SE Geysers Field, California, USA, *Proceedings, World Geothermal Congress 2000*, pp. 2887–2892, International Geothermal Association, May-June, 2000.

Stark, M.A., W.T. Box Jr., J.J. Beall, K.P. Goyal, and A.S. Pingol. The Santa Rosa – Geysers Recharge Project, Geysers Geothermal Field, California,

USA, *Proc. World Geotherm. Cong. 2005*, paper 2420, 2005.

Stark, M. and B. Koenig. Generation Gain in the Northern Geysers Due to Injection-Derived NCG Reduction, *Transactions, Geothermal Resources Council*, Vol. 25, pp. 469–474, 2001.

Truesdell, A.H., J.R. Haizlip, H. Armannsson and F. D'Amore. Origin and Transport of Chloride in Superheated Geothermal Steam, *Geothermics*, Vol. 18, No. 1/2, pp. 295–304, 1989.

van Genuchten, M.Th. A Closed-Form Equation for Predicting the Hydraulic Conductivity of Unsaturated Soils, *Soil Sci. Soc. Am. J.*, Vol. 44, pp. 892 - 898, 1980.